Ore Geology Reviews 101 (2018) 432–436

Contents lists available at ScienceDirect

Ore Geology Reviews

journal homepage: www.elsevier.com/locate/oregeorev

Review

Introduction to the special issue of Mesozoic W-Sn deposits in South China

Mei-Fu Zhou[a,*], Jianfeng Gao[b], Zheng Zhao[c], Wen Winston Zhao[a]

[a] Department of Earth Sciences, University of Hong Kong, Pokfulam Road, Hong Kong, China
[b] State Key Laboratory of Ore Deposit Geochemistry, Institute of Geochemistry, Chinese Academy of Science, Guiyang, China
[c] MLR Key Laboratory of Metallogeny and Mineral Assessment, Institute of Mineral Resources, Chinese Academy of Geological Sciences, Beijing, China

1. Introduction

South China, a world-famous W-Sn metallogenic region, hosts significant numbers of W and Sn deposits. The world's W and Sn reserves are about 3.1 and 12 million tonnes (USGS report), among which South China accounts for around 45% and 11%, respectively (Chen et al., 2015; Sheng et al., 2015; Zhao et al., 2017). Traditionally, W-Sn deposits were thought mostly in the Nanling region of central South China. However, recent discoveries of super-large deposits, such as the Dahutang and Zhuxi deposits in the Yangtze River region of northeastern South China have greatly increased the W reserves in the country (Hu et al., 2017; Huang and Jiang, 2014; Mao et al., 2015; Pan et al., 2017; Wang et al., 2017; Zhao et al., 2017).

The South China Block was formed by amalgamation of the Yangtze Block to the northwest and Cathaysia Block to the southeast during the Neoproterozoic (Zhao et al., 2011). Extensive magmatism in the Mesozoic has generated voluminous granitoids and was associated with W-Sn mineralization (Hu and Zhou, 2012; Hu et al., 2017; Mao et al., 2015; Zhao et al., 2017). Tungsten is chiefly hosted in wolframite and scheelite, and Sn is mainly cassiterite. In the recent past decade, many aspects of Mesozoic W-Sn deposits in South China have been investigated by using modern research techniques. The implementation of deep exploration projects in China (Sino-probe) has led to the discovery of new ore bodies in the deep part of traditional mining districts (e.g., Zhao et al., 2018f). The main W-Sn deposit types are veinlet-disseminated, skarn, and greisen-quartz-vein (Guo et al., 2018b; Huang and Jiang, 2014; Wei et al., 2018; Xie et al., 2018; Zhao et al., 2017). Trace element analysis by in-situ LA-ICP-MS, cassiterite U-Pb dating and high pressure-temperature experiments have been applied in the studies of W-Sn deposits (e.g., Guo et al., 2018a; Zhang et al., 2018a; Zhao and Zhou, 2015; Zhao et al., 2016; Zhao et al., 2018b). Recent studies of W-Sn mineral deposits in South China have advanced our understanding of the distribution and origin of these deposits. This special issue brings together some of the latest information on these topics in 23 papers that deal with many aspects of these Mesozoic W-Sn mineral deposits.

2. Outline of this special issue

This special issue assembled 23 papers covering studies of three types of deposits (Fig. 1): veinlet-disseminated-type, skarn-type, and quartz-vein and greisen type W-Sn deposits in South China (Parts 1–3), comparison of W-Sn and Cu-Pb-Zn polymetallic deposits (Part 4), studies of W/Sn-related granites (Part 5) and deep prospecting of W-Sn deposit (Part 6) as outlined below.

2.1. Part 1: Veinlet-disseminated-type W-Sn deposits

Song et al. (2018) studied the Dahutang W–Cu–Mo deposit and recognized eight hydrothermal stages. Detailed fluid inclusion and H–O isotope analyses show an early W and a late Cu–Mo ore-forming fluid system. The early ore-forming fluids belong to a medium to high temperature, low salinity system, which was likely exsolved from the Late Jurassic granites. Fluorapatite and wolframite may have precipitated first when the temperature dropped from 400° to 320 °C (along with pH increase) at an estimated depth of 7.8 km. This was likely followed by the extensive scheelite mineralization (with fluorite precipitation) that formed huge disseminated/veinlet-type W orebodies when the temperature further dropped to 200 °C (along with pH increase).

Zhang et al. (2018c) identified four types of alteration, including biotite alteration, phyllic alteration, greisenization and silicification closely related to the W mineralization in Dahutang. The mobile element geochemistry effectively differentiated among the four distinct hydrothermal alteration styles. Especially, during alkaline alteration, biotite is a storage of Fe-Mn and acidically decomposed to form wolframite, while apatite as storage of Ca at alkaline alteration, and acidically decomposed to scheelite. They also established a genetic model for tungsten mineralization including superimposed alteration processes (alkaline overprinted by acidic alteration), showing that the superposition of alterations played an important role in the mineralization of the Dahutang giant tungsten deposit.

Zhang et al. (2018b) compared in-situ trace elements of scheelite from the Shimensi veinlet-disseminated deposit and wolframite from the Xihuashan and Piaotang vein-type deposits. The early-stage scheelite and wolframite display significantly negative Eu anomalies and

* Corresponding author.
E-mail address: mfzhou@hku.hk (M.-F. Zhou).

https://doi.org/10.1016/j.oregeorev.2018.07.023
Received 20 July 2018; Accepted 25 July 2018
Available online 27 July 2018
0169-1368/

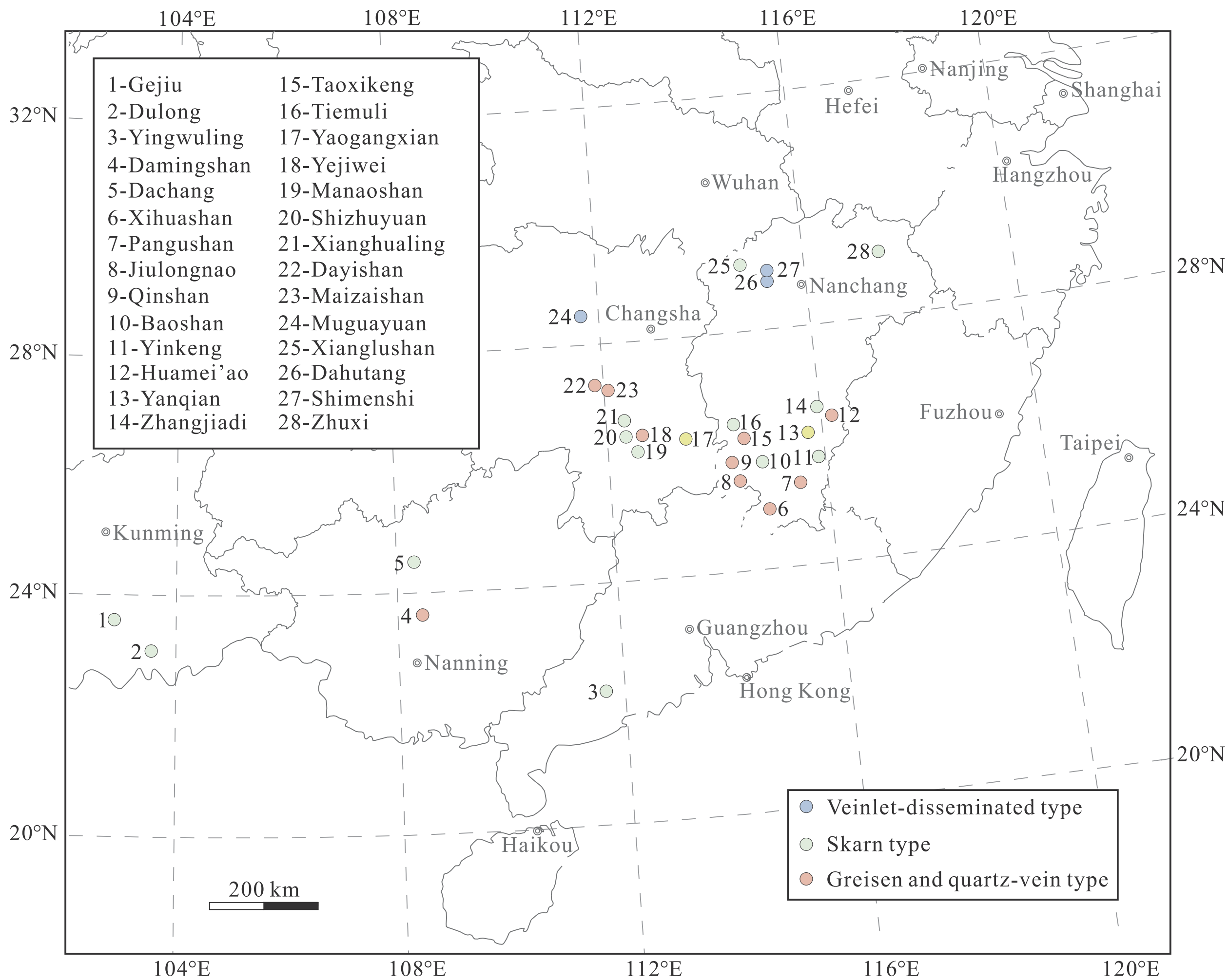

Fig. 1. Distribution of major South China W-Sn deposits in this issue.

have high REE, Nb and Ta contents, suggesting that the initial ore-forming fluids were of magmatic origin. Precipitation of tungsten minerals and alteration would effectively modify the composition of ore-forming fluids. Deposition of the early tungsten minerals would lower REE, Nb and Ta in the mineralizing fluids, leading to depletion of these elements in the late ones. Alteration plays an important role in the formation of veinlet-disseminated scheelite deposits. They concluded that vein-type wolframite mineralization is mainly formed by filling and that veinlet-disseminated scheelite mineralization is associated with metasomatism.

Li et al. (2018b) identified two pulses of ore-forming fluids with different origins and compositions, based on the trace elemental compositions of scheelite and apatite from the Muguanyuan deposit. The early ore-forming fluids, derived from magmas, were relatively reduced with high Mo, Mn, Nb, and Ta, and low Sr, and LREE-enriched with negative Eu anomalies, similar to the regional granitic porphyries. The late fluids, products of mixture between cooled early magmatic fluids and recycled meteoric fluids, were relatively oxidized and Sr-enriched. Extensive greisenization and phyllic alteration led to decomposition of plagioclase providing Ca for scheelite precipitation. They proposed that this mechanism could be popular for granite-hosted, veinlet-disseminated scheelite mineralization in the Jiangnan Orogen.

2.2. Part 2: Skarn-type W-Sn deposits

Zhao and Zhou (2018) reported ages of the three-stage granites in Baoshan granitic pluton are 172.4 Ma, 166.6 Ma, and 156.6 Ma, respectively. The porphyritic granite displays the highest degree of fractionation, which most closely associated with the formation of skarn ores. Also, three stages of skarn formation were recognized. The early prograde stage is mainly composed of Al-rich garnet and Mo-rich scheelite, and typically overgrown by late prograde assemblages of Fe-rich garnet and Mo-depleted scheelite. The retrograde stage is characterized by Al-rich garnet and pure scheelite. The high-temperature and moderate- to high-salinity fluids in the early skarn stages are typical of magmatic fluids originating granites, whereas the lower temperature and variable salinity in the later stages suggest mixing with meteoric water. In addition, this study highlights that the Baoshan skarns show unusual features of "oxidized" skarns overprinted by late "reduced" skarns, which was formed during the subduction of the paleo-Pacific plate in the Jurassic.

Lu et al. (2018) considered that the formation of the Tiemuli skarn-type scheelite-magnetite deposit in the early Cretaceous, at around 135 Ma. Three paragenetic stages of skarn formation have been recognized. Massive magnetite and scheelite orebodies associated with hydrous minerals formed during the retrograde stage. Magma and ore-forming components at Tiemuli were derived mainly from crustal materials, although mafic xenoliths in the granites are consistent with some mantle contribution. The Tiemuli deposit was produced by crust-mantle interaction in an extensional regime, possibly caused by roll-back of the subducting Paleo-Pacific plate during Early Cretaceous. The skarn scheelite and magnetite association formed by interaction between magmatic fluids and calcite-bearing sandstone or impure limestone of the host strata.

Dai et al. (2018) reported, by multiple dating methods, the new ages of the Xianglushan W deposit in northwestern Jiangxi Province. It was formed at ~120 Ma, belonging to the Early Cretaceous W–dominated polymetallic ore-forming event in the Jiangnan porphyry–skarn W belt. The magmatism and mineralization in the Jiangnan porphyry–skarn W belt show that there are two stages of mineralization at 150–135 Ma and 130–120 Ma, respectively. Integrated with published data, it suggests that the Xianglushan W deposit formed in an extensional tectonic setting during the Early Cretaceous.

Zhao et al. (2018c) presented the three phases of the Laojunshan granitic pluton have zircon U-Pb ages of 87.5 Ma, 85.3 Ma, and 82.8 Ma, respectively. Zircon εHf(t) values range from −9.5 to −2.5, showing typical of a mantle origin, whereas trace element patterns are typical of S-type granites. Three main alteration/mineralization stages are recognized as skarn stage, sulfide mineralization stage and supergene stage. Cassiterite U-Pb age of the skarn alteration stage is 89.4 Ma, suggesting that mineralization was associated with the Laojunshan granitic pluton. Regionally, the Sn-polymetallic mineralization in the southwestern South China Block took place within a narrow time span from 97 to 79 Ma. The causative granitic magmas can be produced by partial melting of the Paleoproterozoic–Mesoproterozoic pelitic basement rocks during large-scale lithospheric thinning and asthenospheric upwelling.

Yuan et al. (in press) reported trace elements, especially Sn, concentrations in silicates and oxides from granites and skarns in the world-class Shizhuyuan polymetallic deposit. It shows that Sn is chiefly incorporated in the crystal structures of biotite, garnet, epidote, and magnetite. The following hydrothermal alteration of primary minerals, such as biotite altered to muscovite and/or chlorite, promoted liberation of Sn into magmatic-hydrothermal fluids forming Sn-F complexes, and later precipitated as cassiterite (SnO_2). Finally, it is concluded that the later alteration is the main processes for the formation of Sn ores.

2.3. Part 3 greisen and quartz vein type W-Sn deposits

Zhao et al. (2018e) constrained the Qingshan deposit at the age of ~230 Ma, coeval with the hosting Keshuling pluton, and representing the largest Triassic W(-Sn) polymetallic deposit in South China. During the Triassic, due to the closure of the paleo-Tethys ocean and the subduction of the paleo-Pacific plate, abundant granitic magmas, chiefly derived from the partial melting of crustal materials, were generated under locally extensional settings. The W-enriched magma emplaced mainly in the interior of South China, and formed the main episodes of W(-Sn) mineralization during the Middle to Late Triassic. Their new results suggest that the Triassic large-scale W(-Sn) mineralization occurred throughout the Nanling region.

Wang and Ren (in press) presented a new age of the Yaogangxian tungsten deposit in the central Nanling Range. The overgrowth rims of the zircon grains from the muscovite alkali-feldspar granite and the wolframite-bearing quartz veins have crystallization ages of 133.4 Ma and 133.7 Ma, whereas the relict cores have ages of 155.3 Ma and 154.8 Ma, respectively. The ages of the cores are identical to the crystallization age of the hosting Yaogangxian biotite monzogranite. Thus, these cores were derived from the biotite monzogranite, whereas the overgrowth rims should have crystallized during the intrusion of muscovite alkali-feldspar granite and wolframite-bearing quartz veins. The geochemical consanguinity and similar ages of the muscovite alkali-feldspar granite and the ore veins suggest that they were both formed from the highly-fractionated granitic magma in an extensional setting. This highly-fractionated granitic melt might be extracted from the biotite-monzogranitic mush in a long-surviving deep-seated magma chamber.

Sun et al. (2018) presented a new age of the Maozaishan greisen-quartz vein type Sn deposit in the Dayishan orefield in the central Nanling belt. Cassiterite U-Pb ages, molybdenite Re-Os ages and zircon U-Pb ages, together with the field relationships, provide tight constraints on the Dayishan Sn ore-field mineralization at ~156 Ma. Rhenium contents of the molybdenite suggest that the ore-forming materials were derived from a crustal source, whereas S and Pb isotopic data point to mixed sources. They suggest that the Maozaishan deposit was formed by intrusion of the related pluton, and occurred in the Late Jurassic during a period of lithospheric thinning and crustal extension of the South China Block.

Li et al. (2018a) reported experiments of the dissolution and crystallization of huebnerite in the $MnWO_4$-Li_2CO_3 (or Na_2CO_3)–H_2O system using a hydrothermal diamond-anvil cell (HDAC). The results showed that the weak alkali condition in the carbonate solutions enhanced the crystallization of huebnerite when the temperature and pressure were decreased. The dissolution of $MnWO_4$ mainly attributed to the alkaline environment in the alkali-carbonate aqueous solution. The experimental results indicate that although the crystallization temperature-pressure conditions of huebnerite vary in a wide range, conditions lower than approximately 200 MPa and 450 °C are not favorable for huebnerite crystallization. Our experimental results also suggest that the alkali-carbonate aqueous solution could serve as a medium for the transport of tungsten in the ore-forming process.

2.4. Part 4: Comparison of W-Sn and Cu-Pb-Zn polymetallic deposits

Zhao et al. (2018a) took a systematic geochronological comparison of the Dongpo orefield. This orefield consists of the Shizhuyuan W–Sn–Mo–Bi skarn deposit, Ma'naoshan W–Sn–Fe–Mn–Pb–Zn skarn-greisen deposit, and Yejiwei Sn–Cu deposit and the Pb–Zn–Ag vein-type mineralization. These deposits are all formed contemporaneously at ~151 Ma. Integrating with those of previous studies, the new genetic model of the large-scale accumulation of W–Sn–Mo–Bi–Pb–Zn–Ag in the Dongpo orefield suggests that the proximal skarn-greisen W–Sn–Mo–Bi and distal vein Pb–Zn–Ag mineralization in the Dongpo orefield are genetically related to the Qianlishan pluton and that the mineralization type is mainly controlled by the characteristics of the wall rock.

Guo et al. (2018a) compared the cassiterite U-Pb ages and in-situ trace elements from Tongkeng-Changpo and Gaofeng Sn–Zn–Pb deposits, the Dafulou, Huile and Kangma Sn–Zn deposits. Ages of the five major deposits in the Dachang district, ranging from 90.3 to 95.4 Ma, which agree well with the emplacement age of the biotite granite, is showing a close temporal link between the granitic magmatism and tin-dominant polymetallic mineralization. LA-ICP-MS trace element analyses of cassiterite grains indicate that they have relatively high Ti, Fe and W but low Nb and Ta contents. Combined with Cretaceous U–Pb ages, elevated Fe and W contents of cassiterite suggest tin-dominant polymetallic deposits in the Dachang district were formed in a granite-related magmatic-hydrothermal system controlled by the Longxianggai biotite granite, precluding their syngenetic origin.

Yang et al. (2018) compared the In situ Hf-O-Li isotopic compositions of zircon and Sr-Nd isotopes of apatite, suggesting that the Shuikoushan granitic pluton was likely generated from dehydration melting of amphibolite from a metal-fertile mafic source in the middle-to-lower crust, whereas the Xihuashan granitic pluton could be derived from partial melting of metapelite with minor amphibolite in the middle to upper crust. The geochemical records in accessory minerals fingerprint that the Shuikoushan granitic magma was characterized by high Cl content and $\log fo_2$ value, whereas the Xihuashan granitic magma have elevated F and Li contents with low $\log fo_2$ value, which suggested moderately oxidized magmas with high Cl contents are in favor of the formation of magmatic-hydrothermal Cu-Pb-Zn deposits, whereas weakly reduced magmas with high F and Li contents could be involved in the formation of the quartz vein-type wolframite deposits. In conclusion, different source rocks and magmatic evolution processes are the key to the understanding of the Jurassic diverse granitoid-related mineralization in the Nanling Range.

2.5. Part 5: W/Sn-related granites

Zhao et al. (2018d) documented that the granitic magmatism in the Xingguo orefield lasted for ~8 Mys (ca. 160–153 Ma), whereas the W mineralization occurred in a relatively short period (159–155 Ma), corresponding in age to the episode of large-scale, Mesozoic (165–150 Ma) mineralization in South China. Low εNd(t) values of the Jiangbei granitic rocks and low Re contents of the molybdenite suggest that the W-dominated ores and associated granites in the Xingguo orefield were derived mainly from crustal magmas. The Zr/Hf, Nb/Ta, δEu, Rb/Sr, and LREE/HREE ratios all correlate positively with the W contents of the rocks and reach their highest level in the phase II granites. They propose a magmatic-metallogenic model in which W was concentrated by fractionation of crustally derived magmas of phase I and then deposited in skarn-, greisen-, and quartz vein-type ores by both magmatic and hydrothermal processes.

Wei et al. (2018) reported a new zircon U–Pb ages for the ore-bearing porphyritic biotite granite (151.3 Ma) and fine-grained granite (150.1 Ma and 150.7 Ma), which represent the oldest granitic magmatism reported at Shimensi. The ore-bearing granite porphyry ages (142.7 Ma and 143.3 Ma) have better constrained the timing of the Jurassic-Early Cretaceous ore-forming magmatism. The calculated zircon εHf(t) and δ18Ovalues of the Shimensi granites suggest that the latter were mainly derived from the partial melting of heterogeneous source rocks, probably with combined contributions from the Neoproterozoic Shuangqiaoshan Group metamorphic rocks and Jiuling granodiorite. The calculated zircon Eu/Eu* and Ce4+/Ce3+ ratios of the granites indicate very low oxygen fugacity (fO_2) for the ore-forming magmas, a highly favorable factor for W mineralization. Potentially W and Cu-rich source rocks, and highly-fractionated and reducing granitic magmas, were important factors that triggered the super-large W mineralization at Shimensi.

Guo et al. (2018b) presented a case study of granitic magmatic evolution and W-Sn-Nb-Ta mineralization of the Mesozoic Jiulongnao complex in Nanling region. The four phases of Jiulongnao complex have zircon U-Pb ages of 160.9 ± 0.6 Ma, 158.6 ± 0.7 Ma, 157.0 ± 1.5 Ma and 154.1 ± 1.2 Ma, with TZr of 746–760 °C, 712–802 °C, 798–810 °C, and 648–731 °C, respectively. Oxygen fugacities of Phases I to III display a decreasing trend but Phase IV has much higher oxygen fugacity in its early stage, which decreased in the late stage. The four phases have different accessory mineral assemblages. These mineral assemblages, together with other geological and geochemical features, suggest that W mineralization was genetically related to Phases I, II and IV, whereas U mineralization was most extensive in Phase II. Sn, Nb and Ta mineralization was associated with the highly fractionated of magmas of Phase IV.

Zhang et al. (2018a) presented zircon U–Pb ages of K-feldspar granite, biotite granite and weathered ore-bearing granites, which are around ~79 Ma, in agreement with the cassiterite U–Pb age of 79.6 Ma, indicating a close genetic link between the Yingwuling pluton and W–Sn mineralization. Geochemically, Yingwuling granites belong to shoshonitic series and high-K calc-alkaline series, while the biotite granite experienced a higher degree of fractional crystallization. Their Sr and Nd isotope compositions and zircon Hf isotope values indicates mixing processes of the Yingwuling A-type granitic pluton, formed in an extensional setting. Late Cretaceous W–Sn deposits constitute an EW-trending belt from Guangdong to Yunnan provinces, which was compatible with the northward subduction of the Neo-Tethys plate rather than the northwestward subduction of the Pacific plate during Late Cretaceous.

Xie et al. (2018) reported textural and chemical results of W–Nb–Ta oxide minerals from the Laiziling granitic pluton. The presence of the oxide minerals suggests that the W–Nb–Ta mineralization developed during the latter stages of the magmatic evolution, related to fluids that were compositionally evolved from the granites. The composition of the fluids controls the aggregate of the oxide minerals. The wolframite and cassiterite that precipitated within the Laiziling skarn-type deposit are chemically different from those within the granite, indicating a hydrothermal origin for the oxide minerals that formed as a result of pervasive alteration.

2.6. Part 6: Prospecting of W-Sn deposits

Zhao et al. (2018f) utilized multiple geophysical methods, including gravity, magnetic, audio-frequency magnetotelluric sounding (AMT), and high-resolution reflection seismic techniques, to detect the underground distribution of granites, strata, and ore-controlling structures in the Yinkeng W-Ag-Au-Pb-Zn orefield in the Nanling region. The F1 nappe structure has provided channels for magmas and mineralized hydrothermal fluids, while the slip surface of the nappe equivalent to a depth of more than 4000 m. Specifically, the Gaoshanjiao granodioritic pluton, closely related to precious metal mineralization. The Jiangbei granitic pluton, which typically hosts W mineralization, has lower magnetism that reveals a NE-trending extension about 2.2–2.8 km wide at a depth of 16.6 km. One completely concealed granite, the Yinkeng pluton, lies below the nappe structure, which could represent a good exploration target for porphyry-skarn-type, W-Cu-polymetallic deposits (drilling site for SP-NLSD-1).

Fang et al. (in press) used samples from the Nanling Scientific Drilling (SP-NLSD-2) in the Pangushan W deposit, which has penetrated a zonation from exocontact W-bearing quartz veins to alkali autometasomatic zone and then to primary K-feldspar granite. Multiple dating for the samples separated from the NLID-2(0–2012 m) indicates that the granite emplacement, potassium autometasomatism, greisenization, and W mineralization occurred at ~164.8 Ma, ~161.7 Ma, ~153.8 Ma, and 155.9–152 Ma, respectively. The W mineralization was approximately 9–13 Myr yuonger than the hosting granite. The granite was formed from high-K calcalkaline, metaluminous to peraluminous, highly differentiated magmas that were enriched in W and Bi. The latter occurrence of feldspar quartz vein exhausted K and caused the residual post-magmatic fluids to be rich in Si and W. The evolved post-magmatic fluids formed W-bearing quartz veins with decreasing temperature and pressure. The main reason for W enrichment in the hydrothermal fluids was due to the successive crystallization of minerals rather than autometasomatism.

Acknowledgements

Several research projects made this special issue possible and include grants from the National Key R&D Program of China (2016YFC0600207, 2016YFC0600208), National Science Foundation of China (41372092), a grant from the Research Grant Council of Hong Kong (17306814), and Special Fund for Public Welfare Professions from the Ministry of Land and Resources of the People's Republic of China (No. 201411050). This study is also supported by the "One hundred Talents Plan" grant to Gao JF, and National Nonprofit Institute Research Grant of Chinese Academy of Geological Sciences (No. JYYWF20180502). We thank all of the authors for their contributions in preparing the papers for this special issue within a tight time frame. In addition, we express our sincere thanks to reviewers for their great assistance in a timely fashion.

References

Chen, Z., Sheng, J., Liu, L., Wang, D., Liang, T., Wang, C., 2015. A preliminary review of metallogenic regularity of tin deposits in China. Acta Geol. Sin. English Edit. 89 (3), 1021–1035.

Dai, P., Mao, J., Wu, S., Xie, G., Luo, X., 2018. Multiple dating and tectonic setting of the early cretaceous xianglushan W deposit, Jiangxi Province, South China. Ore Geol. Rev. 95, 1161–1178.

Fang, G., Zhao, Z., Chen, Y., Chen, Z., Krapez, B., Mao, J., in press. Genetic relationship between granitic magmatism and W mineralization recorded in the Nanling Scientific Drilling (SP-NLSD-2) in the Pangushan W mining district, South China, Ore Geology Reviews.

Guo, J., Zhang, R., Sun, W., Ling, M., Hu, Y., Wu, K., Luo, M., Zhang, L., 2018a. Genesis of tin-dominant polymetallic deposits in the Dachang district, South China: Insights from cassiterite U-Pb ages and trace element compositions. Ore Geol. Rev. 95, 863–879.
Guo, N.-X., Zhao, Z., Gao, J.-F., Chen, W., Wang, D.-H., Chen, Y.-C., 2018b. Magmatic evolution and W-Sn-U-Nb-Ta mineralization of the Mesozoic Jiulongnao granitic complex, Nanling Range, South China. Ore Geol. Rev. 94, 414–434.
Hu, R.Z., Zhou, M.F., 2012. Multiple Mesozoic mineralization events in South China—an introduction to the thematic issue. Miner Depos. 47, 579–588.
Hu, R.-Z., Chen, W.T., Xu, D.-R., Zhou, M.-F., 2017. Reviews and new metallogenic models of mineral deposits in South China: an introduction. J. Asian Earth Sci. 137, 1–8.
Huang, L.C., Jiang, S.Y., 2014. Highly fractionated S-type granites from the giant Dahutang tungsten deposit in Jiangnan Orogen, Southeast China: geochronology, petrogenesis and their relationship with W-mineralization. Lithos 202–203 (4), 207–226.
Li, J., Liu, Y., Zhao, Z., Chou, I.-M., 2018a. Roles of carbonate/CO2 in the formation of quartz-vein wolframite deposits: Insight from the crystallization experiments of huebnerite in alkali-carbonate aqueous solutions in a hydrothermal diamond-anvil cell. Ore Geol. Rev. 95, 40–48.
Li, X.-Y., Gao, J.-F., Zhang, R.-Q., Lu, J.-J., Chen, W.-H., Wu, J.-W., 2018b. Origin of the Muguayuan veinlet–disseminated tungsten deposit, South China: constraints from in-situ trace element analyses of scheelite. Ore Geol. Rev.
Lu, L., Liang, T., Zhao, Z., Liu, S., 2018. A Unique association of scheelite and magnetite in the Tiemuli W-Fe skarn deposit: implications for early cretaceous metallogenesis in the Nanling Region, South China. Ore Geol. Rev. 94, 136–154.
Mao, Z.H., Liu, J.J., Mao, J.W., Deng, J., Zhang, F., Meng, X.Y., Xiong, B.K., Xiang, X.K., Luo, X.H., 2015. Geochronology and geochemistry of granitoids related to the giant Dahutang tungsten deposit, middle Yangtze River region, China: Implications for petrogenesis, geodynamic setting, and mineralization. Gondwana Res. 28 (2), 816–836.
Pan, X., Hou, Z., Li, Y., Chen, G., Zhao, M., Zhang, T., Zhang, C., Wei, J., Kang, C., 2017. Dating the giant Zhuxi W-Cu deposit (Taqian–Fuchun Ore Belt) in South China using molybdenite Re–Os and muscovite Ar–Ar system. Ore Geol. Rev. 86, 719–733.
Sheng, J., Liu, L., Wang, D., Chen, Z., Ying, L., Huang, F., Wang, J., Zeng, L., 2015. A preliminary review of metallogenic regularity of tungsten deposits in China. Acta Geol. Sin. English Edit. 89 (4), 1359–1374.
Song, W.-L., Yao, J.-M., Chen, H.-Y., Sun, W.-D., Ding, J.-Y., Xiang, X.-K., Zuo, Q.-S., Lai, C.-K., 2018. Mineral paragenesis, fluid inclusions, H-O isotopes and ore-forming processes of the giant Dahutang W–Cu–Mo deposit, South China. Ore Geol. Rev. 99, 116–150.
Sun, H., Zhao, Z., Yan, G., Lü, Z., Huang, Z., Yu, X., 2018. Geological and geochronological constraints on the formation of the Jurassic Maozaishan Sn deposit, Dayishan orefield, South China. Ore Geol. Rev. 94, 212–224.
Wang, C., Rao, J., Chen, J., Ouyang, Y., Qi, S., Li, Q., 2017. Prospectivity mapping for "Zhuxi-type" copper-tungsten polymetallic deposits in the Jingdezhen region of Jiangxi Province, South China. Ore Geol. Rev. 89, 1–14.
Wang, X., Ren, M., in press. Constraints of hydrothermal and magmatic zircon on the origin of the Yaogangxian tungsten deposit, South China. Ore Geology Reivews.
Wei, W.-F., Shen, N.-P., Yan, B., Lai, C.-K., Yang, J.-H., Gao, W., Liang, F., 2018. Petrogenesis of ore-forming granites with implications for W-mineralization in the super-large Shimensi tungsten-dominated polymetallic deposit in northern Jiangxi Province, South China. Ore Geol. Rev. 95, 1123–1139.
Xie, L., Wang, Z., Wang, R., Zhu, J., Che, X., Gao, J., Zhao, X., 2018. Mineralogical constraints on the genesis of W-Nb–Ta mineralization in the Laiziling granite (Xianghualing district, south China). Ore Geol. Rev. 95, 695–712.
Yang, J.-H., Kang, L.-F., Peng, J.-T., Zhong, H., Gao, J.-F., Liu, L., 2018. In-situ elemental and isotopic compositions of apatite and zircon from the Shuikoushan and Xihuashan granitic plutons: implication for Jurassic granitoid-related Cu-Pb-Zn and W mineralization in the Nanling Range, South China. Ore Geol. Rev. 93, 382–403.
Yuan, J., Hou, Q., Yang, Z., Jiang, H., Hu, Z., Yu, T., in press. LA-ICP-MS analyses reveal tin distribution and mobilization in silicate minerals from the Shizhuyuan tungsten polymetallic deposit, South China. Ore Geology Reviews.
Zhang, L., Zhang, R., Wu, K., Chen, Y., Li, C., Hu, Y., He, J., Liang, J., Sun, W., 2018a. Late Cretaceous granitic magmatism and mineralization in the Yingwuling W-Sn deposit, South China: constraints from zircon and cassiterite U–Pb geochronology and whole-rock geochemistry. Ore Geol. Rev. 96, 115–129.
Zhang, Q., Zhang, R.-Q., Gao, J.-F., Lu, J.-J., Wu, J.-W., 2018b. In-situ LA-ICP-MS trace elemental analyses of scheelite and wolframite: constraints on the genesis of veinlet-disseminated and vein-type tungsten deposits, South China. Ore Geol. Rev.
Zhang, Y., Gao, J.-F., Ma, D., Pan, J., 2018c. The role of hydrothermal alteration in tungsten mineralization at the Dahutang tungsten deposit, South China. Ore Geol. Rev. 95, 1008–1027.
Zhao, J.-H., Zhou, M.-F., Yan, D.-P., Zheng, J.-P., Li, J.-W., 2011. Reappraisal of the ages of Neoproterozoic strata in South China: no connection with the Grenvillian orogeny. Geology 39 (4), 299–302.
Zhao, P., Yuan, S., Mao, J., Yuan, Y., Zhao, H., Zhang, D., Shuang, Y., 2018a. Constraints on the timing and genetic link of the large-scale accumulation of proximal W-Sn–Mo–Bi and distal Pb–Zn–Ag mineralization of the world-class Dongpo orefield, Nanling Range, South China. Ore Geol. Rev. 95, 1140–1160.
Zhao, W.W., Zhou, M.-F., 2015. In-situ LA–ICP-MS trace elemental analyses of magnetite: the mesozoic tengtie skarn fe deposit in the nanling range, South China. Ore Geol. Rev. 65, 872–883.
Zhao, W.W., Zhou, M.-F., 2018. Mineralogical and metasomatic evolution of the Jurassic Baoshan scheelite skarn deposit, Nanling, South China. Ore Geol. Rev. 95, 182–194.
Zhao, W.W., Zhou, M.-F., Chen, W.T., 2016. Growth of hydrothermal baddeleyite and zircon in different stages of skarnization. Am. Mineral. 101 (12), 2689–2700.
Zhao, W.W., Zhou, M.-F., Li, Y.H.M., Zhao, Z., Gao, J.-F., 2017. Genetic types, mineralization styles, and geodynamic settings of Mesozoic tungsten deposits in South China. J. Asian Earth Sci. 137, 109–140.
Zhao, W.W., Zhou, M.-F., Williams-Jones, A.E., Zhao, Z., 2018b. Constraints on the uptake of REE by scheelite in the baoshan tungsten skarn deposit, South China. Chem. Geol. 477, 123–136.
Zhao, Z., Hou, L., Ding, J., Zhang, Q., Wu, S., 2018c. A genetic link between Late Cretaceous granitic magmatism and Sn mineralization in the southwestern South China Block: a case study of the Dulong Sn-dominant polymetallic deposit. Ore Geol. Rev. 93, 268–289.
Zhao, Z., Liu, C., Guo, N.-X., Zhao, W.W., Wang, P.-A., Chen, Z.-H., 2018d. Temporal and spatial relationships of granitic magmatism and W mineralization: Insights from the Xingguo orefield, South China. Ore Geol. Rev. 95, 945–973.
Zhao, Z., Zhao, W.W., Lu, L., Wang, H.-Y., 2018e. Constraints of multiple dating of the Qingshan tungsten deposit on the Triassic W (-Sn) mineralization in the Nanling region, South China. Ore Geol. Rev. 94, 46–57.
Zhao, Z., Zhou, X.-P., Guo, N.-X., Zhang, H.-Y., Liu, Z.-Y., Zheng, Y.-L., Zeng, Z.-L., Chen, Y.-C., 2018f. Superimposed W and Ag-Pb-Zn (-Cu-Au) mineralization and deep prospecting: Insight from a geophysical investigation of the yinkeng orefield, South China. Ore Geol. Rev. 93, 404–412.